THE JOURNAL OF PHYSICAL CHEMISTRY B

Article

pubs.acs.org/JPCB

Template Induced Conformational Change of Amyloid-β Monomer

Wenhui Xi, Wenfei Li,* and Wei Wang*

National Laboratory of Solid State Microstructure, and Department of Physics, Nanjing University, Nanjing 210093, China

Supporting Information

ABSTRACT: Population of aggregation-prone conformers for the monomeric amyloid-β (Aβ) can dramatically speed up its fibrillar aggregation. In this work, we study the effect of preformed template on the conformational distributions of the monomeric Aβ by replica exchange molecular dynamics. Our results show that the template consisting of Aβ peptides with cross-β structure can induce the formation of β-rich conformations for the monomeric Aβ, which is the key feature of the aggregation-prone conformers. Similar effect is observed when the hIAPP peptides and poly alanine peptides were used as templates, suggesting that the template effect is insensitive to the sequence details of the template peptides. In comparison, the template with helical structure has no significant effects on the β-propensity of the monomeric Aβ. Analysis to the interaction details revealed that the template tends to disrupt the intrapeptide interactions of the monomeric Aβ, which are absent in the fibrillar state, suggesting that the preformed template can reorganize the intrapeptide interactions of the monomeric Aβ during the capturing stage and reduce the energy frustrations for the fibrillar aggregations.

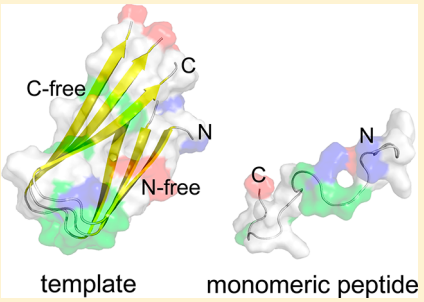

INTRODUCTION

Accumulation of amyloid-β (Aβ) aggregates in the brain is the key pathological feature of the Alzheimer's disease (AD).[1−5] It was widely accepted that the aggregation of the Aβ peptides is involved in the AD pathogenesis.[6,7] Experimental data showed that the structure of the Aβ peptide in the aggregates are dominated by parallel cross-β.[8−11] However, in aqueous solvent, the Aβ is mostly unstructured. Therefore, during the aggregation of the Aβ peptides, the monomer undergoes conformational conversion from random structure to β-strands. In addition, a number of theoretical and experimental works showed that the preformation of the aggregation-prone conformers of the monomeric Aβ peptides, which are rich of β-strands, can significantly speed up the further elongation of the fibrils.[12−19] Undoubtedly, revealing the molecular mechanism of the conformational change of the monomeric Aβ during the aggregation is crucial to understanding the pathology of the AD disease. Particularly, it is interesting to investigate which factors can promote the formation of the aggregation-prone conformer and therefore speed up the fibrillar aggregations.

It was shown that many physical and chemical factors, including pH environment,[20,21] temperature,[22,23] organic solvent,[24−27] mutation,[28] and metal ions[13,29−31] etc., can affect the conformational distribution of the Aβ monomer and enhance the aggregation-prone conformations. For example, in ref 21, using molecular dynamics simulations, Brooks and co-workers observed that modestly acidic pH environment increases the population of the β-turn conformations of the monomeric Aβ, which can further contribute to the fibrillar aggregations. In our previous work, we revealed that binding of divalent metal ions to the N-terminal part of the Aβ monomer promotes the formation of the aggregation-prone conformations.[13] Such works can be highly useful to the understanding of the Aβ aggregation in the cell environment in which Aβ peptides encounter extremely complicated physical and chemical factors.

Recently, a number of works have been devoted to revealing the growth mechanism of the Aβ fibrils.[12,32−41] Particularly, a two-step dock-and-lock mechanism was proposed to interpret the elongation kinetics of the Aβ fibrils.[15] In this mechanism, the disordered Aβ monomer first docks with the fibril end through diffusion-limited kinetics. Then, the Aβ monomer is locked to the fibril by conformational reorganization and forms the correct cross-β structure. Detailed characterizations to the thermodynamics of the above-mentioned docking and locking transitions were reported by Takeda and Klimov in ref 32 and by Han and Hansmann in ref 33 using atomistic molecular dynamics simulations. Although, the monomeric Aβ fully folds to the cross-β structure only after its locking to the growing fibril, it senses the interactions arising from the template peptides during its approaching to the fibril template. Such interactions will no doubt modulate the conformational distribution of the monomeric Aβ before its final locking to the fibril. It is interesting to investigate whether such conformational modulations by the template peptides can promote the formation of the above-mentioned aggregation-prone conformations.

In this work, by using replica exchange molecular dynamics (REMD), we study the effects of the preformed template on the structure of the approaching Aβ monomer. We are interested in the following questions: (i) how the template

Received: January 12, 2012
Revised: May 3, 2012
Published: June 6, 2012

affects the conformational distributions of the approaching monomeric Aβ peptide and (ii) how sensitive is such template effect to the sequence and secondary structure of the template peptides? Our results show that the preformed template with cross-β structure can dramatically increase the β-propensity of the monomeric Aβ. Meanwhile, the interactions arising from the template tend to disrupt the intrapeptide interactions of the monomeric Aβ, which are absent in the fibril, therefore reduces the energy frustration during its fibrillar aggregation. Both effects can promote the fibrillar aggregation of the Aβ peptides. Such template effects are insensitive to the sequence details of the template peptides. In comparison, the template with helical structure has no significant effects on the β-propensity of the monomeric Aβ. Our results add new understanding to the molecular mechanism of the early stage of the Aβ fibrillar aggregation.

MATERIALS AND METHODS

In this work, the simulations were performed using AMBER 11 software[42] and the ff99SB force field.[43] The solvent was taken into account with generalized Born (GB) model.[44,45] The OBC version of the GB model developed in ref 45 was used. To speed up the conformational sampling, we used the REMD method.[46] With this method, the peptides at low temperatures have the ability to overcome the high energy barrier by being switched to higher temperatures, and it provides improved sampling at lower temperatures than the standard MD. The REMD has been widely used in the studies of protein folding and aggregations.[13,47−54] Further details of the REMD can be found in refs 46 and 55. In the simulations, a monomeric Aβ was placed around a preformed structure template, which consists of one Aβ peptide, two Aβ peptides, and three Aβ peptides, respectively (see Figure 1). The backbone dihedral angles and the Cα distances of the template peptides were restrained according to the solid-state NMR structure (ssNMR) (PDB code: 2BEG).[8] In addition, we performed the similar simulations with the template consisting of one Aβ peptide with helical structure. To study the sequence dependence of the template effects, we also conducted the simulations with the template consisting of three hIAPP peptides[56] and the template consisting of three poly alaine peptides, and similar restraints were applied. As a control, the free Aβ peptide without template was conducted. During the simulations, when the distances d of the center of mass (COM) of the monomeric Aβ and the template are larger than 40 Å, a harmonic potential $k(d-40)^2$ with force constant k = 1.0 kcal/(mol·Å^2) was applied to maintain frequent interpeptide interactions. Since the structure information of the N-terminal 1−16 segment of the Aβ peptides is absent in the PDB structure, only the segment 17−42 was included in the current simulations for both the monomeric peptide and the template peptides. It is worth noting that, in the ssNMR structure of the Aβ fibril, the Aβ peptides in the two ends are not equivalent.[8] In one of the end peptides, the side chains of the N-terminal strand (18−26) are more exposed than those of the C-terminal strand (31−42) (see Figure 1). In comparison, the Aβ peptide in the other end exposes the side chains of the C-terminal strand to a larger extent. For convenience, in the following discussions, we designate the end peptides of the template as N-free peptide and C-free peptide, respectively.

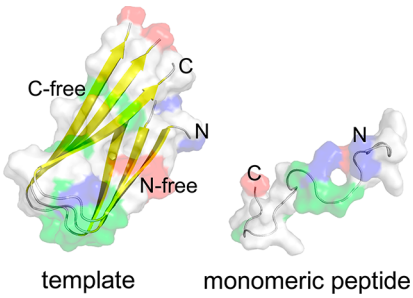

Figure 1. Representative structures of the studied system, including template peptides (left) and monomeric Aβ (right). Only the segment 17−42 was included in the current simulations. The two peptides in the ends of the template were labeled as N-free peptide and C-free peptide, respectively. Color code: white, hydrophobic residues; green, polar residues; blue, positively charged residues; red, negatively charged residues.

We used 32 replicas in each REMD simulation with the temperatures ranging from 280 to 600 K and distributed exponentially. In the simulations, first, the initial structures, which were derived from the PDB structure, were minimized for 1000 steps. Then, the systems were heated to 600 K during the MD simulation of 1.0 ns. The structures of the last 100 ps with COM distances between template and monomeric Aβ larger than 30 Å were used as the initial structures for the REMD simulations. The SHAKE algorithm[57] was used to constrain the covalent bonds involving hydrogen atoms, and a time step of 2 fs was used. The time interval of the exchange attempts in the REMD was set as 1.5 ps. Snapshot coordinates were recorded every 0.75 ps for further analysis. For each replica, the MD simulation length is 204 ns, which leads to an accumulative simulation time of 6.5 μs for each of the REMD simulations.

In analyzing the data, the structures of the first 60 ns were omitted. The secondary structure of each residue was assigned based on its backbone dihedral angles following the PROSS algorithm.[58,59] In the calculations of the contact maps, the contacts are considered as formed whenever two amino acid side chains, which are separated by at least four amino acids, have any two heavy atoms within 5.0 Å. Similarly, a hydrogen bond is defined as formed when the distance between the donor and acceptor is less than 3.5 Å, and the donor−hydrogen−acceptor angle is larger than 120.0°. To characterize the structure details of the sampled conformations, conformational clustering was conducted for the structures sampled at 325 K. The average-linkage algorithm[60] was used in the clustering analysis with the structure similarity measured by root-mean-square deviation (rmsd) of the heavy atoms.

RESULTS AND DISCUSSION

Effect of Template on Conformational Distribution of the Monomeric Aβ. To investigate how the preformed structure template affects the conformational distribution of the monomeric Aβ, we compared the populations of the β-strand conformations for each residue of the monomeric Aβ with and without the presence of the preformed structure template. Figure 2a shows the percentage of the β-strand conformation sampled by the residues of the monomeric Aβ with (black) and without (blue) the preformed structure template at the temperature of 325 K. The same results for the temperature of 300 K were shown in the Figure S1 of the Supporting Information. To test possible convergence of the simulations, we divided the full data sampled at each temperature into ten groups with equal time duration and calculated the percentage

dx.doi.org/10.1021/jp300389g | J. Phys. Chem. B 2012, 116, 7398−7405

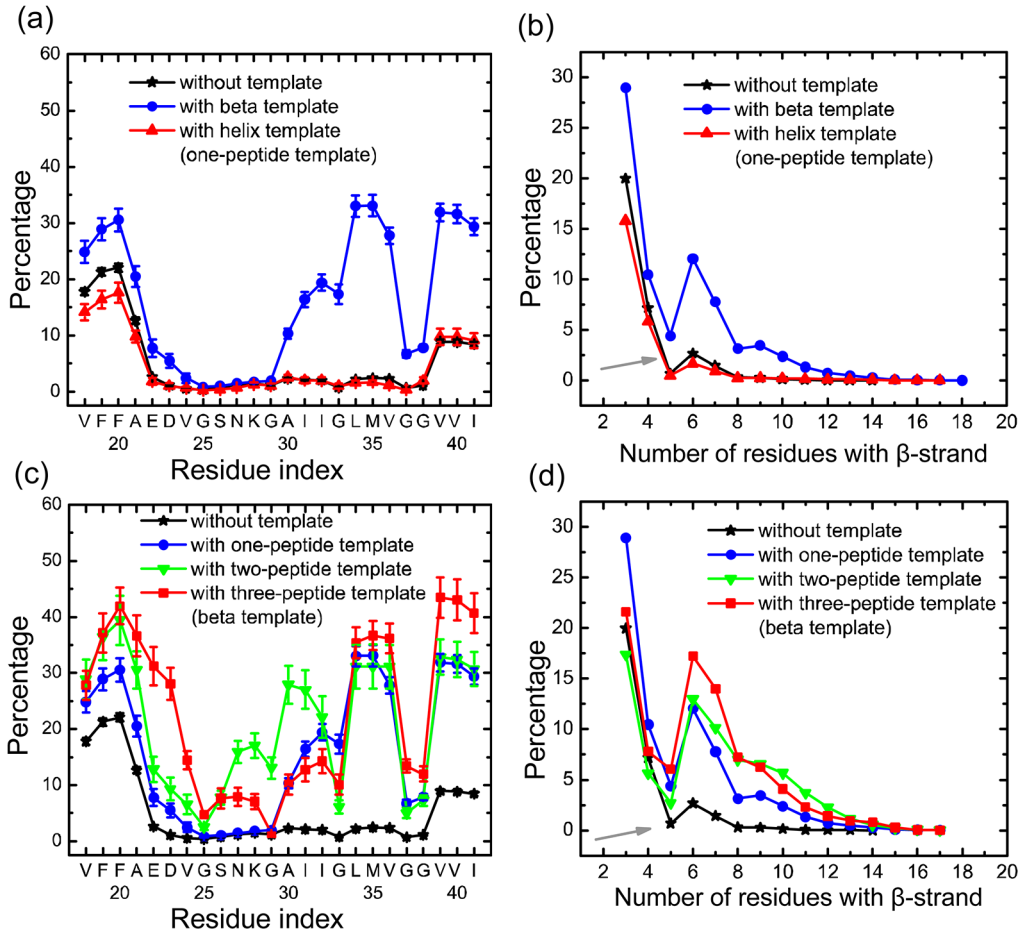

Figure 2. (a) Percentage of the β-strand conformation sampled by the residues of the monomeric Aβ with the one-peptide template of different secondary structures at 325 K. Color code: blue, β template; red, helix template. For comparison, the results without a template were also shown (black). (b) The distribution of the number of residues with β conformation for the one-peptide template case. (c) Percentage of the β-strand conformation sampled by the residues of the monomeric Aβ with the two-peptide template (green) and three-peptide template (red) of cross-β structure at 325 K. The results with the one-peptide template (blue) and without template (black) were also shown for comparison. (d) Similar to that in panel b but with the helix template being changed to the two-peptide template and three-peptide template. The small percentages around the arrow in panels b and d result from the definitions of the β-strand conformation in PROSS, which demands three or more consecutive residues satisfying the dihedral angle constraints.

for each of the groups. The error bars in Figure 2 represent the standard errors calculated from the results of different groups. The small error bars suggest that the sampling in this work is reasonably converged for the comparison of the β-strand percentages. Here, the structure template consists of one Aβ peptide, and its structure was restrained according to the ssNMR structure (i.e., with β-strand conformation). For comparison, we also show the results for the structure template with helical conformation (red). One can see that the template with β-strand conformation enhances the β-propensity of the monomeric Aβ significantly. Particularly, the β-propensities of the segments 17−21 and 30−41, which have high β-content in the fibrils, were enhanced more drastically. Similar effects can be inferred from the right shifting of the distribution of the number of residues with β-strand shown in Figure 2b. In comparison, the template with helical conformation has almost no effect on the β-propensity of the monomeric Aβ, except that the β-propensity of the segment 17−21 is decreased to some extent. Instead, the helix template tends to increase the helical propensity of the monomeric Aβ as shown in the Figure S2 of the Supporting Information. Since the β-rich conformations are more prone to fibrillar aggregation, the above results suggest that the preformed structure template with β-strand conformations tends to promote the formation of aggregation-prone conformations for the monomeric Aβ. Such effect of preformed structure template on the conformational distributions of the monomeric Aβ can be highly relevant to the Aβ fibrillation. It was well established that the accumulation of the aggregation-prone conformers would results in an enhanced tendency to aggregate.[12] Therefore, the above observed effect of template suggests that the preformed structure template with cross-β structure tends to enhance the Aβ fibrillar aggregation. Particularly, such effects are sensitive to the secondary structure of the template peptides.

It is not surprising to observe the above template effects. It is highly possible that such template effects can play important roles during the folding of proteins. For example, the similar effects of the secondary structure template on the folding of the poly alanine peptides were observed based on MD simulations by Takada and co-workers.[55] Particularly, they demonstrated that the helix template enhances the helical propensity of the surrounding peptide by lowering the nearby dielectric constant.

In the above discussions, the template consists of only one Aβ monomer. Such template tends to form hydrogen bonds

dx.doi.org/10.1021/jp300389g | J. Phys. Chem. B 2012, 116, 7398−7405

with the monomeric Aβ mostly along the lateral direction as demonstrated in Figure 3a, which shows the representative

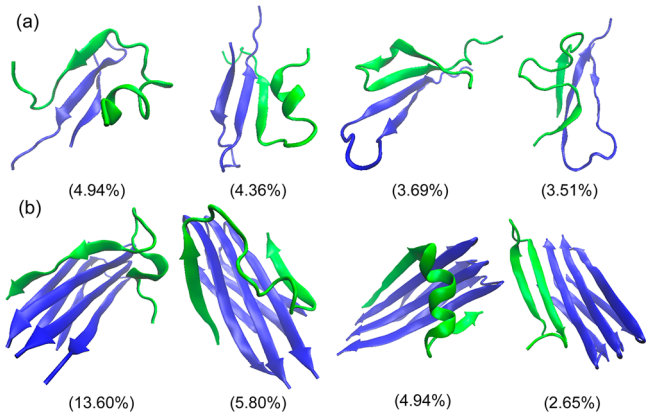

Figure 3. Representative structures of the most populated four clusters for the one-peptide template (a) and three-peptide template simulations (b) at 325 K. The relative sizes of the clusters were presented in the brackets. The template peptides are colored in blue, and the monomeric Aβ are colored in green.

structures of the most populated four clusters obtained by clustering analysis. However, in the amyloid fibrils, the newly added Aβ monomers form hydrogen bonds with the preformed fibril along the fibril axis. To more realistically describe the template effects of the preformed fibril template, we also conducted simulations with a template containing two and three Aβ peptides, and their conformations were restrained to cross-β structure according to the ssNMR data.[8] Figure 2c shows the percentage of the β-stand conformation sampled by each residue of the monomeric Aβ with the two-peptide template (green) and three-peptide template (red). For comparison, the results without a template (black) and with the one-peptide template (blue) are also shown. One can see that both the two-peptide template and three-peptide template have basically similar effects on the β-propensities as that of the one-peptide template (see also Figure 2d). However, compared to the one-peptide template, the two-peptide template and three-peptide template increase the β-propensities more drastically (Figure 2c,d). Compared to the one-peptide template, the two-peptide template has a larger effect around the residues 25−32. In contrary, the three-peptide template has a larger effect around residues 20−25 and residues 39−41. However, from the current simulation results, we cannot observe clear trend of the template effects on the conformational distributions as the number of template peptides increases. In Figure 3b, we also show the representative structures of the most populated four clusters for the three-peptide template. We can see that the monomeric Aβ forms hydrogen bonds to the template with very different ways between the one-peptide template and the three-peptide template. As discussed above, in the one-peptide template case, the monomeric Aβ forms hydrogen bonds with the template mostly along the lateral direction. In comparison, in the three-peptide template case, the monomeric Aβ forms hydrogen bonds along the fibril axis. Such difference suggests that during the nucleation stage of the Aβ aggregation, conformational conversion from lateral β-sheet to axial β-sheet is the necessary step. As the conformational conversion from lateral β-sheet to axial β-sheet involves the breaking and reforming of a large number of hydrogen bonds, it needs to overcome a high energy barrier. Therefore, such conformational conversion may contribute to the lag time in the initial stage of the Aβ fibrillar aggregation observed experimentally.[61]

To further understand the effects of the template on the conformational distributions of the Aβ monomer, it is important to study the changes of the interaction details within the monomeric Aβ induced by the template. Figure 4 shows the contact map and hydrogen map of the monomeric Aβ without template (a,b) and with the one-peptide (c,d) and three-peptide templates (e,f), respectively. For clarity, the contact map and hydrogen map for the simulations with one-peptide template and three-peptide template are shown by the probability differences relative to the simulation without template (c-f). Blue color represents that the template reduces the intrapeptide contacts. In contrary, the red color represents that the template enhances the intrapeptide contacts. One can see that the intrapeptide contacts are disrupted significantly with the presence of the template. Without template, the 1−4 hydrogen bonds are formed with high probability, which indicates the high populations of the helical conformation. With the presence of the template, the numbers of 1−4 intrapeptide hydrogen bonds are much reduced. Such effect is more pronounced for the three-peptide template. These results suggest that, during the capturing stage, the template tends to disrupt the intrapeptide interactions of the approaching monomeric Aβ. Since these 1−4 hydrogen bonds are mostly absent in the fibril state, the reduction of the intrapeptide interactions can be helpful for eliminating the energy frustrations during the fibrillar aggregation, and optimizing the interactions between the monomeric Aβ and the growing fibril. Consequently, the energy landscape of the monomeric Aβ can be reshaped by the template to favor the fibrillar aggregation. We also calculated the distributions of the total nonlocal energy within the monomeric Aβ with different templates by analyzing the REMD simulation data with the MM/GBSA method[62] implemented in AMBER software, and the results were given in Figure S3 of the Supporting Information. We can see that, for the simulations with templates consisting of peptides with β structure, the nonlocal interactions within the monomeric Aβ are much weaker, which is consistent with the above discussions based on the contact maps.

Interaction Details between the Monomeric Aβ and the Template. According to the two-step mechanism of the fibril elongation, the monomeric Aβ first docks to the growing fibril. Then, it is locked to the fibril by formation of the correct interpeptide hydrogen bonds. Although the current MD simulations are not long enough to cover the whole dock and lock steps, it can still provide useful information on the very initial stage of the capturing process. Here, we mainly focus on the interaction features during the initial stage of the capturing process. More detailed discussions on the thermodynamics of the docking and locking transitions were reported in refs 32 and 33 by using very similar methodologies.

Figure 5a shows the contact probability of each residue in the monomeric Aβ with the template peptides, including the C-free peptide (green), N-free peptide (red), and all the peptides (blue). Similarly, Figure 5b shows the contact probability of each residue in the template peptides (C-free peptide (green), N-free peptide (red), and centric peptide (blue)) with the monomeric Aβ. We can see that the monomeric Aβ interacts differently with the N- and C-terminal segments of the template

dx.doi.org/10.1021/jp300389g | J. Phys. Chem. B 2012, 116, 7398−7405

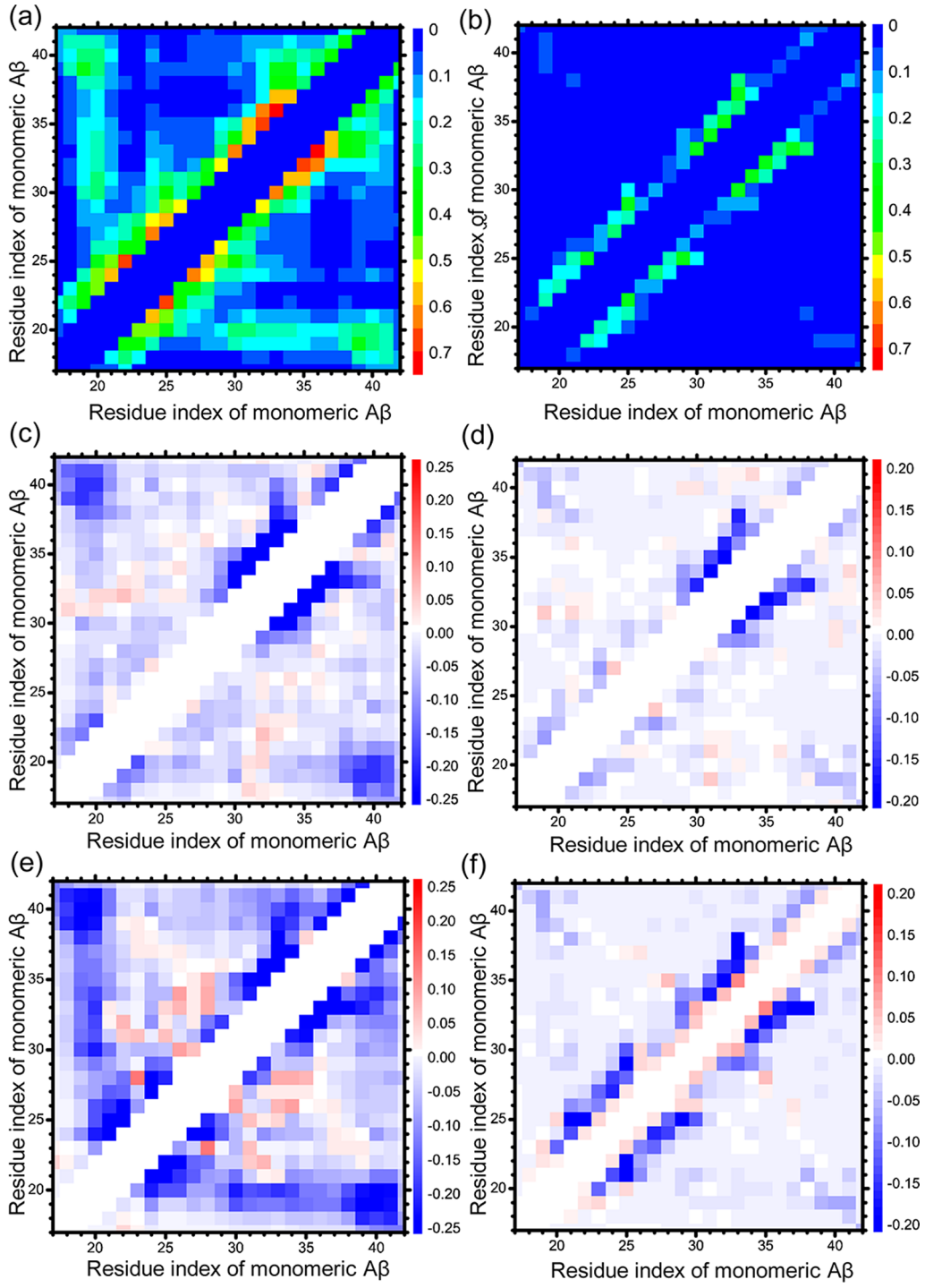

Figure 4. Contact map (left) and hydrogen map (right) of the monomeric Aβ without a template (a,b) and with the one-peptide (c,d) and three-peptide templates (e,f) at 325 K. In panel a, the contact map represents the formation probabilities of the contacts between each pair of residues. In panel b, the hydrogen map represents the formation probabilities of the hydrogen bonds between the backbone groups of each pair of residues. In panels c–f, the contact maps and hydrogen maps are shown by the probability differences relative to the simulation without a template.

peptides. The interactions involving the C-terminal segment of the template peptides are much more probable (Figure 5b). Particularly, the interpeptide interactions are dominated by the segment 31–37 of the template peptides, which are highly hydrophobic. One can also notice that the interpeptide contacts occur mainly in the hydrophobic residues of the N- and C-terminal segments. In comparison, the loop part, which consists of polar and charged residues, forms less interpeptide contacts. Such results may suggest that the hydrophobic interactions play a crucial role in the capturing of the monomeric Aβ by the template.

We can also observe that the N-free peptide and C-free peptide of the template interact with the monomeric Aβ differently (Figure.5b). The monomeric Aβ forms more contacts with the N-free peptide of the template (red). Interestingly, such interaction polarity was also proposed in other computational studies.[32,33] In comparison, the centric peptide in the template contributes much less to the

dx.doi.org/10.1021/jp300389g | J. Phys. Chem. B 2012, 116, 7398–7405

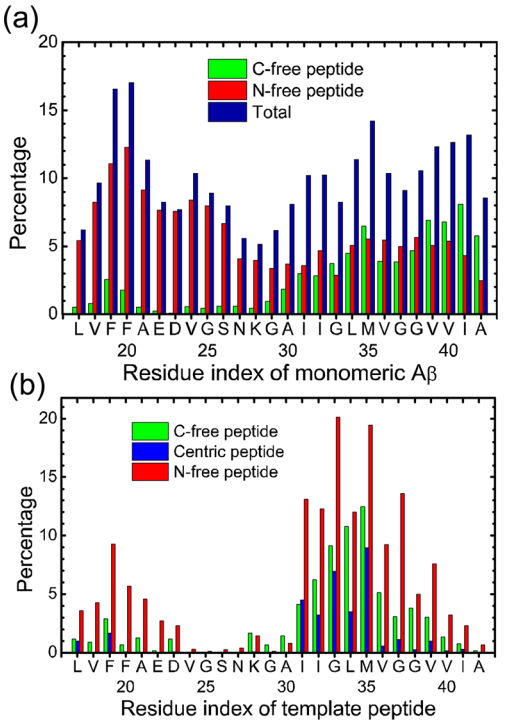

Figure 5. (a) Contact probability of each residue in the monomeric Aβ with the C-free peptide (green), N-free peptide (red), and all the peptides (blue) of the three-peptide template at 325 K. (b) Contact probability of the C-free peptide (green), N-free peptide (red), and centric peptide (blue) in the three-peptide template with the monomeric Aβ at 325 K.

interpeptide interactions (Figure 5b), probably due to its limited accessibility to the monomeric Aβ since it is mostly packed by the end peptides. It is not surprising to observe such interaction polarity since the structures of the end peptides are not equivalent in the ssNMR structure as discussed in the Methods section. The end peptides expose the side chains in the N-terminal β-strand and C-terminal β-strand to different extents, which results in the different interactions with the monomeric Aβ.

Sequence Dependence of the Template Effects. The above results demonstrated that the preformed structure template can promote the formation of the aggregation-prone conformations before the monomeric Aβ finally locks to the growing fibril, and such template effect strongly depends on the secondary structure of the template peptides. It is also interesting to investigate whether such template effect is sensitive to the sequence details of the template peptides. For this purpose, we conducted similar simulations but with the template consisting of hIAPP peptides. The fibrillar aggregation of the hIAPP is considered to be crucial for the type-II diabetes.[63−65] Similar to the Aβ peptide, the hIAPP is rich of hydrophobic residues. Figure 6 shows the percentage of the β-strand conformation sampled by the residues of the monomeric Aβ with the hIAPP template (blue) and Aβ template (red). For comparison, we also show the results without template (black). One can see that, both the hIAPP and the Aβ templates tend to enhance the β-propensity of the monomeric Aβ, indicating that the observed template effects are not very sensitive to the sequence details of the template peptides when the residues of the template is hydrophobic enough. As discussed in ref 61, the sequences of hIAPP and Aβ share some common features as

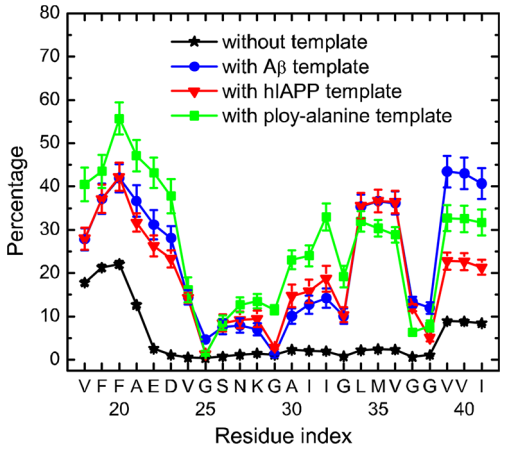

Figure 6. Percentage of the β-strand conformation sampled by the residues of the monomeric Aβ with the Aβ template (red), hIAPP template (blue), and poly alanine template (green) at 325 K. The results without a template (black) were also shown for comparison.

indicated by the high sequence similarity (~50%). To further eliminate the sequence correlation, we designed an artificial template consisting of three poly alanine peptides (by replacing the side-chains of the three-peptide Aβ template with methyl groups). The backbone structure is restrained to the same cross-β structure as that in the three-peptide Aβ template. The results show that, even for such a special peptide with sequence significantly different from that of the Aβ peptide, the β-propensity of the monomeric Aβ peptide can be improved to a large extent (Figure 6, green). Such observation further supports the argument that the template effects are not very sensitive to the sequence details of the template peptides. The above results suggest that the deposition of the fibrillar aggregates with a certain sequence may be able to promote the aggregation of other peptides with different sequence. Interestingly, it was observed experimentally[61] that the preformed hIAPP fibrils can enhance the fibrillation of the free Aβ peptide, which indicates the cross-seeding of the fibrillar aggregation. The results of the current simulations are consistent with the experimental observations. Such cross-seeding phenomenon has also been suggested in other experimental works,[66] and it was considered to be relevant to the infections of some amyloid diseases.[67]

■ CONCLUSIONS

We studied the effects of the preformed structure template on the conformational distributions of the monomeric Aβ peptide using atomistic simulations. Our results showed that the template with the cross-β structure is able to induce the formation of β-rich conformations for the monomeric Aβ. Such effect is insensitive to the sequence details of the template peptides but strongly depends on the secondary structure of the template peptides. In addition, the template tends to disrupt the intrapeptide interactions of the monomeric Aβ, which is absent in the fibril state, and therefore reduces the energy frustrations in the final locking stage of the fibrillar aggregation. Our results suggest that the structure of the monomeric Aβ is susceptible to the interactions from the fibril template. As the monomeric Aβ approaches the preformed fibril, its conformation is reorganized by the interactions arising from the template peptides, which results in the populations of aggregation-prone conformations, and contributes to the growth of the fibrils.

dx.doi.org/10.1021/jp300389g | J. Phys. Chem. B 2012, 116, 7398−7405

It is worth noting that the time scale of the current MD simulations is far below the time scale of the whole dock and lock steps, as also noted by the authors in ref 33. Therefore, the conformations sampled in the current simulations mostly represent the events that occurred during the very initial stage of the attachment. The drastic effects of the template on the conformational distributions of the monomeric Aβ observed in this work strongly indicate that the preformed template begin to reshape the energy landscape of the monomeric Aβ in the very early stage of the aggregation.

■ ASSOCIATED CONTENT

Supporting Information

Percentage of the β-strand conformation sampled by the residues of the monomeric Aβ; percentage of the helical conformation sampled by the residues of the monomeric Aβ; distributions of intra-peptide nonlocal energy for the monomeric A. This material is available free of charge via the Internet at http://pubs.acs.org.

■ AUTHOR INFORMATION

Corresponding Author

*E-mail: wfli@nju.edu.cn (W.L.); wangwei@nju.edu.cn (W.W.).

Notes

The authors declare no competing financial interest.

■ ACKNOWLEDGMENTS

We thank the Shanghai Supercomputer Center and High Performance Computing Center of Nanjing University for the computational support. This work was supported by the National Natural Science Foundation of China (Grants Nos. 10704033, 11174134, 91127026, and 11111140012), Natural Science Foundation of Jiangsu Province (Grants Nos. BK2011546 and BK2009008), and PAPD.

■ REFERENCES

(1) Selkoe, D. J. *Physiol. Rev.* **2001**, *81*, 741−766.
(2) Finder, V. H.; Glockshuber, R. *Neurodegener. Dis.* **2007**, *4*, 13−27.
(3) Blennow, K.; de Leon, M. J.; Zetterberg, H. *Lancet* **2006**, *368*, 387−403.
(4) Rauk, A. *Chem. Soc. Rev.* **2009**, *38*, 2698−2715.
(5) Chiti, F.; Dobson, C. M. *Annu. Rev. Biochem.* **2006**, *75*, 333−366.
(6) Hardy, J.; Selkoe, D. J. *Science* **2002**, *297*, 353−356.
(7) LaFerla, F. M.; Green, K. N.; Oddo, S. *Nat. Rev. Neurosci.* **2007**, *8*, 499−509.
(8) Luhrs, T.; Ritter, C.; Adrian, M.; Riek-Loher, D.; Bohrmann, B.; Doeli, H.; Schubert, D.; Riek, R. *Proc. Natl. Acad. Sci. U.S.A.* **2005**, *102*, 17342−17347.
(9) Petkova, A. T.; Yau, W.-M.; Tycko, R. *Biochemistry* **2005**, *45*, 498−512.
(10) Tycko, R. *Annu. Rev. Phys. Chem.* **2011**, *62*, 279−299.
(11) Tycko, R. *Q. Rev. Biophys.* **2006**, *39*, 1−55.
(12) Straub, J. E.; Thirumalai, D. *Annu. Rev. Phys. Chem.* **2011**, *62*, 437−463.
(13) Li, W. F.; Zhang, J.; Su, Y.; Wang, J.; Qin, M.; Wang, W. *J. Phys. Chem. B* **2007**, *111*, 13814−13821.
(14) Esler, W. P.; Stimson, E. R.; Ghilardi, J. R.; Vinters, H. V.; Lee, J. P.; Mantyh, P. W.; Maggio, J. E. *Biochemistry* **1996**, *35*, 749−757.
(15) Esler, W. P.; Stimson, E. R.; Jennings, J. M.; Vinters, H. V.; Ghilardi, J. R.; Lee, J. P.; Mantyh, P. W.; Maggio, J. E. *Biochemistry* **2000**, *39*, 6288−6295.
(16) Ban, T.; Yamaguchi, K.; Goto, Y. *Acc. Chem. Res.* **2006**, *39*, 663−670.
(17) Harper, J. D.; Lieber, C. M.; Lansbury, P. T. *Chem. Biol.* **1997**, *4*, 951−959.
(18) Petkova, A. T.; Leapman, R. D.; Guo, Z. H.; Yau, W. M.; Mattson, M. P.; Tycko, R. *Science* **2005**, *307*, 262−265.
(19) Bellesia, G.; Shea, J. E. *J. Chem. Phys.* **2009**, *130*, 145103.
(20) Ma, K.; Clancy, E. L.; Zhang, Y. B.; Ray, D. G.; Wollenberg, K.; Zagorski, M. G. *J. Am. Chem. Soc.* **1999**, *121*, 8698−8706.
(21) Khandogin, J.; Brooks, C. L. *Proc. Natl. Acad. Sci. U.S.A.* **2007**, *104*, 16880−16885.
(22) Kusumoto, Y.; Lomakin, A.; Teplow, D. B.; Benedek, G. B. *Proc. Natl. Acad. Sci. U.S.A.* **1998**, *95*, 12277−12282.
(23) Danielsson, J.; Jarvet, J.; Damberg, P.; Graslund, A. *FEBS J.* **2005**, *272*, 3938−3949.
(24) Hamada, D.; Dobson, C. M. *Protein Sci.* **2002**, *11*, 2417−2426.
(25) Wang, S. S. S.; Chen, Y. T.; Chen, P. H.; Liu, K. N. *Biochem. Eng. J.* **2006**, *29*, 129−138.
(26) Klimov, D. K.; Straub, J. E.; Thirumalai, D. *Proc. Natl. Acad. Sci. U.S.A.* **2004**, *101*, 14760−14765.
(27) Wei, G. H.; Shea, J. E. *Biophys. J.* **2006**, *91*, 1638−1647.
(28) Baumketner, A.; Krone, M. G.; Shea, J. E. *Proc. Natl. Acad. Sci. U.S.A.* **2008**, *105*, 6027−6032.
(29) Miller, Y.; Ma, B. Y.; Nussinov, R. *Proc. Natl. Acad. Sci. U.S.A.* **2010**, *107*, 9490−9495.
(30) Tougu, V.; Tiiman, A.; Palumaa, P. *Metallomics* **2011**, *3*, 250−261.
(31) Drago, D.; Bolognin, S.; Zatta, P. *Curr. Alzheimer Res.* **2008**, *5*, 500−507.
(32) Takeda, T.; Klimov, D. K. *Biophys. J.* **2009**, *96*, 442−452.
(33) Han, M.; Hansmann, U. H. E. *J. Chem. Phys.* **2011**, *135*, 065101.
(34) Auer, S.; Dobson, C. M.; Vendruscolo, M.; Maritan, A. *Phys. Rev. Lett.* **2008**, *101*, 258101.
(35) Bernstein, S. L.; Dupuis, N. F.; Lazo, N. D.; Wyttenbach, T.; Condron, M. M.; Bitan, G.; Teplow, D. B.; Shea, J. E.; Ruotolo, B. T.; Robinson, C. V.; Bowers, M. T. *Nat. Chem.* **2009**, *1*, 326−331.
(36) Massi, F.; Straub, J. E. *Proteins: Struct., Funct., Bioinf.* **2001**, *42*, 217−229.
(37) Reddy, G.; Straubb, J. E.; Thirumalai, D. *Proc. Natl. Acad. Sci. U.S.A.* **2009**, *106*, 11948−11953.
(38) Nguyen, P. H.; Li, M. S.; Stock, G.; Straub, J. E.; Thirumalai, D. *Proc. Natl. Acad. Sci. U.S.A.* **2007**, *104*, 111−116.
(39) Buchete, N. V.; Hummer, G. *Biophys. J.* **2007**, *92*, 3032−3039.
(40) Wu, C.; Lei, H. X.; Duan, Y. *J. Am. Chem. Soc.* **2005**, *127*, 13530−13537.
(41) Krone, M. G.; Hua, L.; Soto, P.; Zhou, R. H.; Berne, B. J.; Shea, J. E. *J. Am. Chem. Soc.* **2008**, *130*, 11066−11072.
(42) Case, D. A.; Darden, T. A.; Cheatham, T. E., III; Simmerling, C. L.; Wang, J.; Duke, R. E.; Luo, R.; Walker, R. C.; Zhang, W.; Merz, K. M.; Roberts, B. P.; Wang, B.; Hayik, S.; Roitberg, A.; Seabra, G.; Kolossvai, I.; Wong, K. F.; Paesani, F.; Vanicek, J.; Liu, J.; Wu, X.; Brozell, S. R.; Steinbrecher, T.; Gohlke, H.; Cai, Q.; Ye, X.; Wang, J.; Hsieh, M.-J.; Cui, G.; Roe, D. R.; Mathews, D. H.; Seetin, M. G.; Sagui, C.; Babin, V.; Luchko, T.; Gusarov, S.; Kovalenko, A.; Kollman, P.A. *AMBER 11*; University of California: San Francisco, CA, 2010.
(43) Duan, Y.; Wu, C.; Chowdhury, S.; Lee, M. C.; Xiong, G. M.; Zhang, W.; Yang, R.; Cieplak, P.; Luo, R.; Lee, T.; Caldwell, J.; Wang, J. M.; Kollman, P. *J. Comput. Chem.* **2003**, *24*, 1999−2012.
(44) Qiu, D.; Shenkin, P. S.; Hollinger, F. P.; Still, W. C. *J. Phys. Chem. A* **1997**, *101*, 3005−3014.
(45) Onufriev, A.; Bashford, D.; Case, D. A. *J. Phys. Chem. B* **2000**, *104*, 3712−3720.
(46) Sugita, Y.; Okamoto, Y. *Chem. Phys. Lett.* **1999**, *314*, 141−151.
(47) Li, W. F.; Qin, M.; Tie, Z. X.; Wang, W. *Phys. Rev. E* **2011**, 84.
(48) Takeda, T.; Klimov, D. K. *J. Phys. Chem. B* **2009**, *113*, 11848−11857.
(49) Jiang, P.; Xu, W. X.; Mu, Y. G. *PLoS Comput. Biol.* **2009**, *5*, 1000357.
(50) Garcia, A. E. *Polymer* **2004**, *45*, 669−676.
(51) Sgourakis, N. G.; Yan, Y. L.; McCallum, S. A.; Wang, C. Y.; Garcia, A. E. *J. Mol. Biol.* **2007**, *368*, 1448−1457.

(52) Li, W. F.; Zhang, J.; Wang, J.; Wang, W. *J. Am. Chem. Soc.* **2008**, *130*, 892−900.
(53) Zhang, J.; Li, W. F.; Wang, J.; Qin, M.; Wu, L.; Yan, Z. Q.; Xu, W. X.; Zuo, G. H.; Wang, W. *IUBMB Life* **2009**, *61*, 627−643.
(54) Gnanakaran, S.; Nussinov, R.; Garcia, A. E. *J. Am. Chem. Soc.* **2006**, *128*, 2158−2159.
(55) Zhou, R. H. *J. Mol. Graphics* **2004**, *22*, 451−463.
(56) Luca, S.; Yau, W. M.; Leapman, R.; Tycko, R. *Biochemistry* **2007**, *46*, 13505−13522.
(57) Ryckaert, J. P.; Ciccotti, G.; Berendsen, H. J. C. *J. Comput. Phys.* **1977**, *23*, 327−341.
(58) Srinivasan, R.; Rose, G. D. *Proc. Natl. Acad. Sci. U.S.A.* **1999**, *96*, 14258−14263.
(59) Gong, H. P.; Isom, D. G.; Srinivasan, R.; Rose, G. D. *J. Mol. Biol.* **2003**, *327*, 1149−1154.
(60) Shao, J. Y.; Tanner, S. W.; Thompson, N.; Cheatham, T. E. *J. Chem. Theory Comput.* **2007**, *3*, 2312−2334.
(61) O'Nuallain, B.; Williams, A. D.; Westermark, P.; Wetzel, R. *J. Biol. Chem.* **2004**, *279*, 17490−17499.
(62) Srinivasan, J.; Cheatham, T. E.; Cieplak, P.; Kollman, P. A.; Case, D. A. *J. Am. Chem. Soc.* **1998**, *120*, 9401−9409.
(63) Hoppener, J. W. M.; Lips, C. J. M. *Int. J. Biochem. Cell Biol.* **2006**, *38*, 726−736.
(64) Kahn, S. E.; Andrikopoulos, S.; Verchere, C. B. *Diabetes* **1999**, *48*, 241−253.
(65) Jaikaran, E.; Clark, A. *Biochim. Biophys. Acta, Mol. Basis Dis.* **2001**, *1537*, 179−203.
(66) Vishveshwara, N.; Liebman, S. W. *BMC Biol.* **2009**, *7*, 26.
(67) Haan, M. N. *Nat. Clin. Pract. Neurol.* **2006**, *2*, 159−166.